Lawrence Berkeley National Laboratory
Climate & Ecosystems

Title
Molecular mechanisms of water table lowering and nitrogen deposition in affecting greenhouse gas emissions from a Tibetan alpine wetland

Permalink
https://escholarship.org/uc/item/5vh9n4cn

Journal
Global Change Biology, 23(2)

ISSN
1354-1013

Authors
Wang, Hao
Yu, Lingfei
Zhang, Zhenhua
et al.

Publication Date
2017-02-01

DOI
10.1111/gcb.13467

Peer reviewed

Molecular mechanisms of water table lowering and nitrogen deposition in affecting greenhouse gas emissions from a Tibetan alpine wetland

HAO WANG[1,2], LINGFEI YU[3], ZHENHUA ZHANG[2], WEI LIU[2], LITONG CHEN[2], GUANGMIN CAO[2], HAOWEI YUE[4], JIZHONG ZHOU[4,5,6], YUNFENG YANG[4], YANHONG TANG[1] and JIN-SHENG HE[1,2]

[1] Department of Ecology, College of Urban and Environmental Sciences and Key Laboratory for Earth Surface Processes of the Ministry of Education, Peking University, 5 Yiheyuan Road, Beijing 100871, China, [2] Key Laboratory of Adaptation and Evolution of Plateau Biota, Northwest Institute of Plateau Biology, Chinese Academy of Sciences, 23 Xining Road, Xining 810008, China, [3] State Key Laboratory of Vegetation and Environmental Change, Institute of Botany, Chinese Academy of Sciences, 20 Nanxincun, Beijing 100093, China, [4] State Key Joint Laboratory of Environment Simulation and Pollution Control, School of Environment, Tsinghua University, 1 Tsinghua Garden Road, Beijing 100084, China, [5] Department of Microbiology and Plant Biology, Institute for Environmental Genomics, University of Oklahoma, Norman, OK 73019, USA, [6] Earth Sciences Division, Lawrence Berkeley National Laboratory, Berkeley, CA 94720, USA

Correspondence: Jin-Sheng He, e-mail: jshe@pku.edu.cn

Abstract

Rapid climate change and intensified human activities have resulted in water table lowering (WTL) and enhanced nitrogen (N) deposition in Tibetan alpine wetlands. These changes may alter the magnitude and direction of greenhouse gas (GHG) emissions, affecting the climate impact of these fragile ecosystems. We conducted a mesocosm experiment combined with a metagenomics approach (GeoChip 5.0) to elucidate the effects of WTL (-20 cm relative to control) and N deposition (30 kg N ha^{-1} yr^{-1}) on carbon dioxide (CO_2), methane (CH_4) and nitrous oxide (N_2O) fluxes as well as the underlying mechanisms. Our results showed that WTL reduced CH_4 emissions by 57.4% averaged over three growing seasons compared with no-WTL plots, but had no significant effect on net CO_2 uptake or N_2O flux. N deposition increased net CO_2 uptake by 25.2% in comparison with no-N deposition plots and turned the mesocosms from N_2O sinks to N_2O sources, but had little influence on CH_4 emissions. The interactions between WTL and N deposition were not detected in all GHG emissions. As a result, WTL and N deposition both reduced the global warming potential (GWP) of growing season GHG budgets on a 100-year time horizon, but via different mechanisms. WTL reduced GWP from 337.3 to -480.1 g CO_2-eq m^{-2} mostly because of decreased CH_4 emissions, while N deposition reduced GWP from 21.0 to -163.8 g CO_2-eq m^{-2}, mainly owing to increased net CO_2 uptake. GeoChip analysis revealed that decreased CH_4 production potential, rather than increased CH_4 oxidation potential, may lead to the reduction in net CH_4 emissions, and decreased

nitrification potential and increased denitrification potential affected N_2O fluxes under WTL conditions. Our study highlights the importance of microbial mechanisms in regulating ecosystem-scale GHG responses to environmental changes.

Introduction

Carbon dioxide (CO_2), methane (CH_4) and nitrous oxide (N_2O) are three major greenhouse gases (GHGs) that contribute to the anthropogenic greenhouse effect (IPCC, 2013). Wetlands play a dual role in affecting the atmospheric budgets of these GHGs. Waterlogged conditions lead to significant carbon (C) accumulation because of limited decomposition, which exerts a cooling effect on climate (Frolking *et al*., 2006; Yuan *et al*., 2015). Meanwhile, low redox potentials are conducive to CH_4 and N_2O emissions, which have a warming effect on climate (Smith *et al*., 2003; Frolking *et al*., 2006). Human activities and climate change have resulted in numerous environmental changes, including water table lowering (WTL) in wetlands (Dise, 2009). However, it still remains unclear how the GHG emissions and their net climate impact respond to these changes (Petrescu *et al*., 2015).

The water table is the key factor controlling the boundary between oxic and anoxic soils (Dinsmore *et al*., 2009) and has aroused considerable concern in peatlands and marshes in boreal (Aurela *et al*., 2007; Chivers *et al*., 2009), temperate (Webster *et al*., 2013; Yang *et al*., 2013) and subtropical zones (Malone *et al*., 2013). As the water table lowers, on the one hand, soil CO_2 emission increases because of accelerating organic matter decomposition (Aurela *et al*., 2007; Webster *et al*., 2013). On the other hand, water stress may reduce plant photosynthesis, leading to a decrease in CO_2 uptake (Chivers *et al*., 2009; Malone *et al*., 2013). Meanwhile, WTL also reduces CH_4 production and enhances CH_4 oxidation due to elevated soil oxygen content (Smith *et al*., 2003; Karbin *et al*., 2015), as well as stimulates N_2O emissions because of increased nitrogen (N) availability associated with N mineralization (Goldberg *et al*., 2010).

N deposition is another issue directly linked to wetland GHG emissions. N deposition affects CO_2 fluxes by increasing plant productivity, improving the chemical quality of litter (lower C/N ratio) and alleviating N constraints on microbial metabolism (Bragazza *et al*., 2006; Lebauer & Treseder, 2008). N also alters CH_4 emissions through impacts on microbes and plants, because N influences the activity of methanogens and methanotrophs (Liu & Greaver, 2009), and affects plant productivity and species composition involved in CH_4 production, oxidation and transport (Joabsson *et al*., 1999; Bubier *et al*., 2007; Lai *et al*., 2014). In addition, N input increases N_2O emissions by supplying available N for nitrifying and denitrifying bacteria (Dalal *et al*., 2003; Lohila *et al*., 2010). More importantly, nutrient status has been observed to modulate the effect of WTL on GHG emissions in northern

peatlands (Martikainen *et al*., 1993; Aerts & Ludwig, 1997); however, few studies have investigated the interactive effects of WTL and N deposition in alpine wetlands.

Currently, our understanding of GHG emissions is constrained by limited knowledge of microbial mediated mechanisms (McCalley *et al*., 2014). For CH_4 and N_2O, the linked processes of production and consumption involve methanogens and methanotrophs, as well as nitrifying and denitrifying bacteria (Le Mer & Roger, 2001; Dalal *et al*., 2003). However, determining the roles of these microbes in mediating GHG emissions under WTL and N deposition is difficult. The recently developed microarray-based metagenomics tool (GeoChip 5.0) enables the detection of over 144000 gene sequences from 393 gene families associated with biogeochemical processes (Wang *et al*., 2014a). For example, the CH_4 production potential of methanogens is detected by *mcrA* gene encoding methyl coenzyme M reductase A (Luton *et al*., 2002). The CH_4 oxidation potential of methanotrophs is detected by *pmoA* and *mmoX* genes. The nitrification potential is detected by *amoA* gene encoding ammonia monooxygenase and *hao* gene encoding hydroxylamine oxidoreductase. The denitrification potential is detected by *narG* gene encoding nitrate reductase, *nirS* and *nirK* genes encoding nitrite reductase, and *norB* gene encoding nitric oxide reductase (Yue *et al*., 2015). Therefore, GeoChip 5.0 offers an unprecedented opportunity to investigate the links between microbial functional potentials connected with these processes and net CH_4 or N_2O emissions (Yang *et al*., 2014b).

The aim of this study is to explore how and by what mechanisms GHG fluxes respond to WTL and N deposition in the alpine wetlands of the Tibetan Plateau, which play an important role in regulating regional GHG budget and are subjected to intensified human activities and rapid climate change (Chen *et al*., 2013). Over the past five decades, the wetlands in this plateau (with the exception of riverine and lacustrine wetlands) have undergone widespread degradation (Zhang *et al*., 2011b; Chen *et al*., 2013) that has largely been ascribed to artificial drainage for cultivation (An *et al*., 2007; Zhang *et al*., 2011a) or permafrost degradation associated with climate warming (Cheng & Wu, 2007; Piao *et al*., 2010; Zhang *et al*., 2011b). Meanwhile, this plateau has experienced increasing N deposition (Liu *et al*., 2015), particularly in the northeastern region, where N deposition rates (including dry and wet deposition) have ranged from 4 to 13.8 kg N ha^{-1} yr^{-1} (Lu & Tian, 2007; Fang *et al*., 2012). Although several studies have reported that CH_4 emissions are affected by water table (Chen *et al*., 2008, 2009; Yang *et al*., 2014a; Song *et al*., 2015), or N deposition (Gao *et al*., 2014) in this fragile ecosystem, no study to date has focused on the effects of these changes on net climate impact of GHG emissions and the molecular mechanisms underlying GHG responses.

We hypothesize that WTL decreases net CO_2 uptake and CH_4 emissions but increases N_2O emissions (hypothesis I), since aerobic conditions accelerate

organic matter decomposition, decrease CH_4 production, increase CH_4 oxidation, and provide more available N for nitrification and denitrification by stimulating N mineralization. We also hypothesize that N deposition increases net CO_2 uptake as well as CH_4 and N_2O emissions (hypothesis II), since increased N availability favors nitrifying and denitrifying bacteria and stimulates plant growth under N-limited conditions. Consequently, increased plant productivity could supply more substrate for CH_4 production and more conduits for CH_4 transport. Finally, we hypothesize that N deposition modulates the effects of WTL on GHG fluxes (hypothesis III). WTL could physiologically threaten the function (e.g. the production and consumption of GHGs) of soil microbes by imposing a lower environmental water potential (Schimel *et al*., 2007). N deposition would reduce the WTL-induced negative impact on the microbial function because more N can be used to synthesize chaperones and osmolytes (Csonka, 1989; Yerbury *et al*., 2005). In addition, we quantified the effect of WTL and N deposition on the global warming potential (GWP) of three GHGs on a 100-year time horizon. Using a metagenomics technique, this study is the first to investigate whether variations in CH_4 and N_2O emissions align with that of functional genes associated with CH_4 production and oxidation, nitrification and denitrification in a Tibetan wetland.

Materials and methods

Study site and mesocosm collection

This study was conducted at the Luanhaizi wetland (37°35′N latitude, 101°20′E longitude, 3250 m a.s.l.), located in the northeastern part of the Tibetan Plateau. This area is characterized by a continental monsoon climate, with short, cool summers and long, cold winters. From 1981 to 2010, the mean annual air temperature was −1.1 °C; the mean annual precipitation was 480 mm, and more than 80% of the precipitation was concentrated in the growing seasons (May to September). The wetland is dominated by the vascular plant *Carex pamirensis* and dotted with *Carex atrofusca*, *Hippuris vulgaris*, *Triglochin palustre* and *Heleocharis* spp (Fig. 1a). In the 0- to 10-cm soil layer of the wetland, the soil pH, total C and N content are 7.7, 16.2% and 1.1%, respectively. The local level of atmospheric N deposition ranges from 8.7 to 13.8 kg N ha^{-1} yr^{-1} (Fang *et al*., 2012).
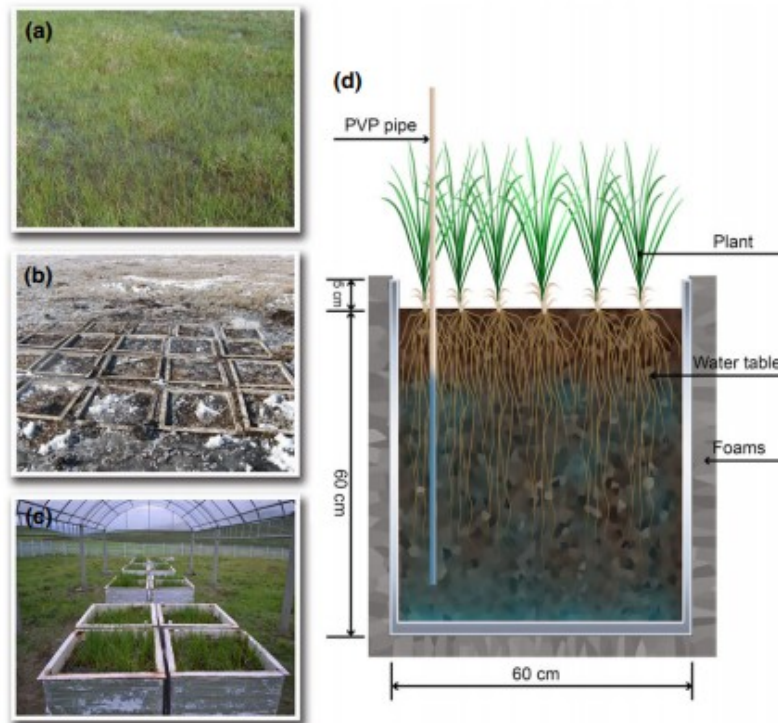
Fig. 1 The landscape of the Luanhaizi wetland in the growing season (a), mesocosm collection in the non-growing season (b), experimental arrangement (c) and sketch map of experiment system (d).

A homogeneous area was selected for mesocosm collection. Twenty bottomless tanks (0.6 m length × 0.6 m width × 0.65 m height, $n = 20$) were inserted into the wetland soil in September 2010, which is close to the end of the growing season. After the soil froze at the end of October, the tanks were excavated (Fig. 1b), the bottom of the tanks was welded, and the outside of the tanks was wrapped with polystyrene foam to avoid heat exchange with their surroundings. To eliminate rain effects on the maintenance of the water table, the mesocosms were placed under a rainfall shelter that is approximately 1000 m away from the excavated site. The rainfall shelter was constructed with anti-ultraviolet plastic transparent plates (Fig. 1c). We let the mesocosms recover from collection and transportation until May 2011 by maintaining the water table at the same depth as that of the natural wetland.

Experimental design

Two water table levels and two N deposition levels were applied in a complete factorial design (2 water table × 2 N deposition). Each treatment had five replicates; twenty mesocosms were randomly arranged into five blocks. Two water table levels (WT^0, 3 cm above the soil surface, and WT$^-$, 20 cm below the soil surface) simulated the present and future water table.

Two N deposition levels (N^0, 0 kg N ha^{-1} yr^{-1} addition; N^+, 30 kg N ha^{-1} yr^{-1} addition) mimicked the scenario of doubled N deposition.

The control water table was set to 3 cm above the soil surface, which was in line with the mean water table under natural growing season conditions. Because the lowest water table at this wetland dropped to approximately 20 cm below the soil surface in the 2010 growing season, the water table in the WTL plots was set to this water level. Wetland water was automatically supplemented by micropumps to control the water table accurately. Manostat systems connected to the micropumps (PULANDI 1205 Diaphragm Pump, Pulandi Machine Equipment Co., Shijiazhuang, China) were used to regulate the water table. When the water table was below the set points, the micropumps turned on and supplemented the tanks with wetland water transported from where the mesocosms were collected. Simulated N deposition was divided into four portions and applied monthly during the growing seasons from 2011 to 2013. The N deposition plots were sprayed with ammonium nitrate (NH_4NO_3) mixed with 1 L of water from the wetland, while the no-N deposition plots were sprayed with the same amount of water without NH_4NO_3.

GHG fluxes measurements

CO_2 fluxes

Net ecosystem CO_2 exchange (NEE) was measured with a transparent chamber (0.4 m length × 0.4 m width × 0.6 m height; without bottom) using an infrared gas analyzer (IRGA; LI-6400, LI-COR Inc., Lincoln, NE, USA). This method has been used and validated in a number of previous studies (e.g. Niu *et al*., 2008). Before the measurements, square collars (0.4 m length × 0.4 m width × 0.1 m height) were inserted 5 cm below the soil surface. During each measurement, the chamber was placed on the collar and sealed with water. A fan was fixed on the top of the sampling chamber to mix the air. Six consecutive values of CO_2 concentration were recorded at 10-s intervals during a measurement period of 1 min after steady-state conditions were reached. The CO_2 flux rate was calculated by the slope of linear regression of the six records in the time series of concentration. After the NEE measurements, we ventilated the chamber, replaced it on the same square collar, and finally covered it with an opaque cloth. These obtained values represent the ecosystem respiration (ER). Gross ecosystem productivity (GEP) was calculated by subtracting ER from NEE. Positive and negative values of CO_2 fluxes indicate CO_2 release and uptake, respectively. We measured CO_2 fluxes twice or thrice per month on sunny days between 9:00 and 12:00 local time for all treatments. We observed the diurnal patterns at 2-h intervals on 21 June, 14 July, 21 August and 6 September 2012.

CH$_4$ and N$_2$O fluxes

CH$_4$ and N$_2$O fluxes were measured according to Yu *et al*. (2013) using static opaque chamber and gas chromatography. The chambers were made of stainless steel and consisted of removable cover boxes (0.4 m length × 0.4 m width × 0.4 m height; without bottom) and square collars. The square collars were the same as those for the CO$_2$ measurements. A fan in each opaque chamber was used to mix the air during sampling. Gas samples were collected at 10-min intervals over 30 min using plastic syringes. Samples were stored in syringes following sampling and subsequently analyzed via gas chromatograph (Agilent 7890A, Agilent Co., Santa Clara, CA, USA) within 24 h. The chromatograph was equipped with a flame ionization detector (FID) to analyze the CH$_4$ concentration and an electron capture detector (ECD) to analyze the N$_2$O concentration (Wang & Wang, 2003). The carrier gas was N$_2$, and the operation temperature for the FID was set at 250 °C and ECD at 300 °C. CH$_4$ and N$_2$O fluxes were calculated by the slopes of linear regressions between gas concentrations and sampling time (0, 10, 20 and 30 min after chamber closure). The coefficients of determination (R^2) of the linear regressions were sometimes low for N$_2$O (<0.4). To avoid a bias from omitting low fluxes, we kept those values when CH$_4$ concentrations showed a good linear trend with time as described by Dijkstra *et al*. (2013). Sampling was conducted twice or thrice per month between 9:00 and 12:00 local time for all treatments, and the diurnal patterns were measured on 26 June, 29 July, 21 August and 1 September 2012. CH$_4$ fluxes were measured from 2011 to 2013, and N$_2$O fluxes were measured in 2012 and 2013.

GWP

Daily fluxes were calibrated as the ratios of daily average values to daytime (9:00–12:00) average values. The calibration coefficients were 0.25 for NEE, 0.91 for ER, 0.86 for CH$_4$ and 0.98 for N$_2$O based on the diurnal patterns of CO$_2$, CH$_4$ and N$_2$O fluxes of the control plots in 2012 (Figs S4 and S5). Seasonal cumulative GHG fluxes were calculated by multiplying the average daily fluxes between two consecutive sampling dates by the time interval, and then by summing up the daily fluxes for all time intervals during the growing seasons. We further assessed the climate impact of growing season GHG budgets using the GWP, which is defined as time-integrated radiative forcing. The 100-year GWP (in g CO$_2$-eq m^{-2}), which was adopted by the UNFCCC and the Kyoto Protocol, was calculated by adding the GWP from NEE, CH$_4$ (seasonal cumulative CH$_4$ fluxes in g CH$_4$ m^{-2} multiplied by 28) and N$_2$O (seasonal cumulative N$_2$O fluxes in mg N$_2$O m^{-2} multiplied by 265 × 10^{-3}) (IPCC, 2013). It should be noted that the GWP in 2011 was calculated only by NEE and CH$_4$; however, the GWP showed no large differences because of the small contribution of N$_2$O (<5% in 2012–2013).

Water table depth and soil temperature measurements

While GHGs were sampled, water table depth and soil temperature at 10 cm depth were recorded. A slotted 2.5 cm diameter polyvinyl chloride pipe was

installed in each tank to measure water table depth (Fig. 1d). No significant changes in soil temperature at 10 cm depth were observed under WTL and N deposition conditions using portable temperature probes (JM 624 Digital Thermometer, Jinming Instrument Co., Ltd., Tianjin, China) (Fig. S1).

Estimation of aboveground net primary production and belowground biomass

The height and density of the plants were measured in the mesocosms during August in 2011, 2012 and 2013. A simulated method was used to estimate the aboveground net primary production (ANPP) nondestructively (Wang *et al.*, 2012). To develop the simulation model, the height and density of the plants in 0.4 m length × 0.4 m width quadrats in the natural wetland were measured, and the aboveground biomass was harvested, dried and weighed in August 2012. Based on the measurements from the natural wetland, a linear equation was established to simulate aboveground plant biomass (APB): APB = $-9.375 + 0.089\ A + 0.972\ H$ ($P < 0.001$, $R^2 = 0.93$, $n = 41$), where A is the total amount of plant stems and H is the mean plant height. The APB in each mesocosm was estimated using this equation to represent the annual ANPP because APB peaks in mid-August in this area.

Upon the completion of the experiment in September 2013, one soil core of 5.0 cm in diameter from each mesocosm was collected to a depth of 50 cm and washed with sieves. Live and dead roots were dried and weighed, and belowground biomass was estimated by the ratio of the live standing root crops to the total root biomass (0.56).

Soil sampling, DNA extraction and GeoChip 5.0 experiments

In mid-September 2013, three soil cores of 5.0 cm in diameter from a depth of 0−50 cm were randomly collected in each mesocosm and then well mixed as a composite soil sample by soil depth (0−10 cm, 10−20 cm, 20−30 cm and 30−50 cm). The soil samples were kept on ice before transportation to the laboratory. Soil samples were then sieved using 2-mm mesh to remove the plant roots and stones and preserved at −80 °C before DNA extraction. Soil samples of 0−10 cm were used for GeoChip 5.0 experiments because the topsoil was significantly affected by WTL and N deposition. Soil DNA was extracted using the MoBio PowerSoil DNA isolation kit (MoBio Laboratories, Carlsbad, CA, USA) according to the manufacturer's instructions. The DNA was further purified by precipitation with ethanol and then dissolved in nuclease-free water. Approximately 0.6 μg of community DNA was labeled with the fluorescent dye Cy-3 and hybridized with GeoChip 5.0 at 67 °C for 24 h in an Agilent hybridization oven. Then, GeoChip microarrays were scanned using a NimbleGen MS200 scanner (Roche, Madison, WI, USA). The detailed descriptions of DNA extraction, purification, labeling, hybridization to GeoChip 5.0, raw data processing and statistical analyses were reported in a previous study (Wang *et al.*, 2014a).

Data analysis

Repeated-measures analysis of variance was used to test the effects of the main factors on CO_2, CH_4, N_2O and ANPP, with water table and N deposition as between-subject factors and year as a within-subject factor, including interactions. Repeated-measures analysis of variance was also used to examine the effects of the main factors on CO_2, CH_4 and N_2O fluxes within each year, with water table and N deposition as between-subject factors and sampling date as a within-subject factor, including interactions. We used post hoc tests (Tukey HSD) to test the differences among treatments. A paired test was used to analyze the effect of water table across different N deposition levels and the effect of N deposition across different water table levels. All statistical analyses were conducted using SPSS 16.0 (SPSS Inc., Chicago, IL, USA).

Results

Aboveground net primary production and belowground biomass

Over the three years of the mesocosm experiment, WTL had no detectable effect on ANPP compared with the no-WTL plots (Fig. 2a). However, the effect of WTL varied with time, with a decrease (16.0%) in 2011, no changes in 2012 and an increase (13.7%) in 2013. Overall, N deposition enhanced ANPP by 11.5% across different water table levels (Fig. 2b). Additionally, this enhancement varied during the study period, with no effect on ANPP in 2011, an increase of 15.5% in 2012, and an increase of 12.4% in 2013.
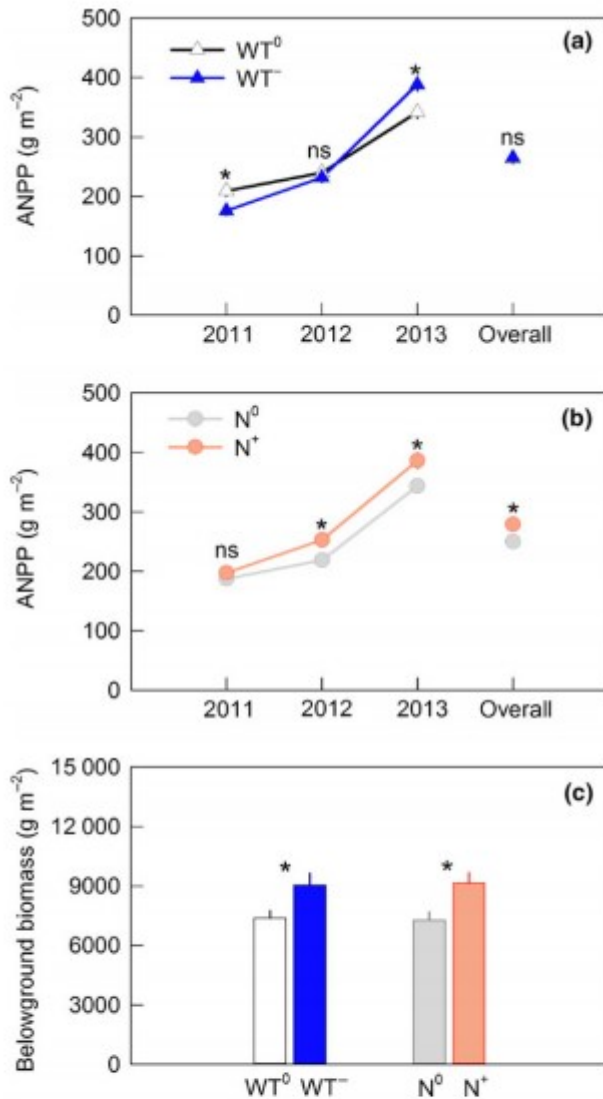
Fig. 2 Effects of water table lowering and nitrogen deposition on aboveground net primary production (ANPP) in 2011–2013 (a, b) and on belowground biomass in September 2013 (c). Bars show $\pm$ SE ($n = 10$). WT^0 and WT^- indicate no water table lowering and water table lowering across different nitrogen deposition levels, respectively. N^0 and N^+ indicate no nitrogen deposition and nitrogen deposition across different water table levels, respectively. ns and *: not statistically significant and statistically significant at $P < 0.05$.

At the end of the experiment, WTL significantly increased belowground biomass by 22.6% in comparison of the no-WTL plots, and N deposition elevated belowground biomass by 25.7% compared with the no-N deposition plots (Fig. 2c).

Carbon dioxide fluxes

GEP was higher than ER, leading to a net CO_2 absorption of 1019.1 g CO_2 m^{-2} averaged by the three consecutive growing seasons (Fig. 3a–c). Seasonal

CO_2 flux dynamics ($P < 0.001$) were observed within each year (Table 1), and CO_2 fluxes peaked in July or August. Although WTL did not significantly affect net CO_2 uptake because of simultaneous increases in ER and GEP across the three years (Table 2), the effect varied with time and the trend changed from negative to positive in August 2012 (Fig. S2a). In comparison with the no-N deposition plots, N deposition elevated the net CO_2 uptake across the three years with an average increase of 25.2%, because of a smaller increase in ER than in GEP (Fig. S2a–c).
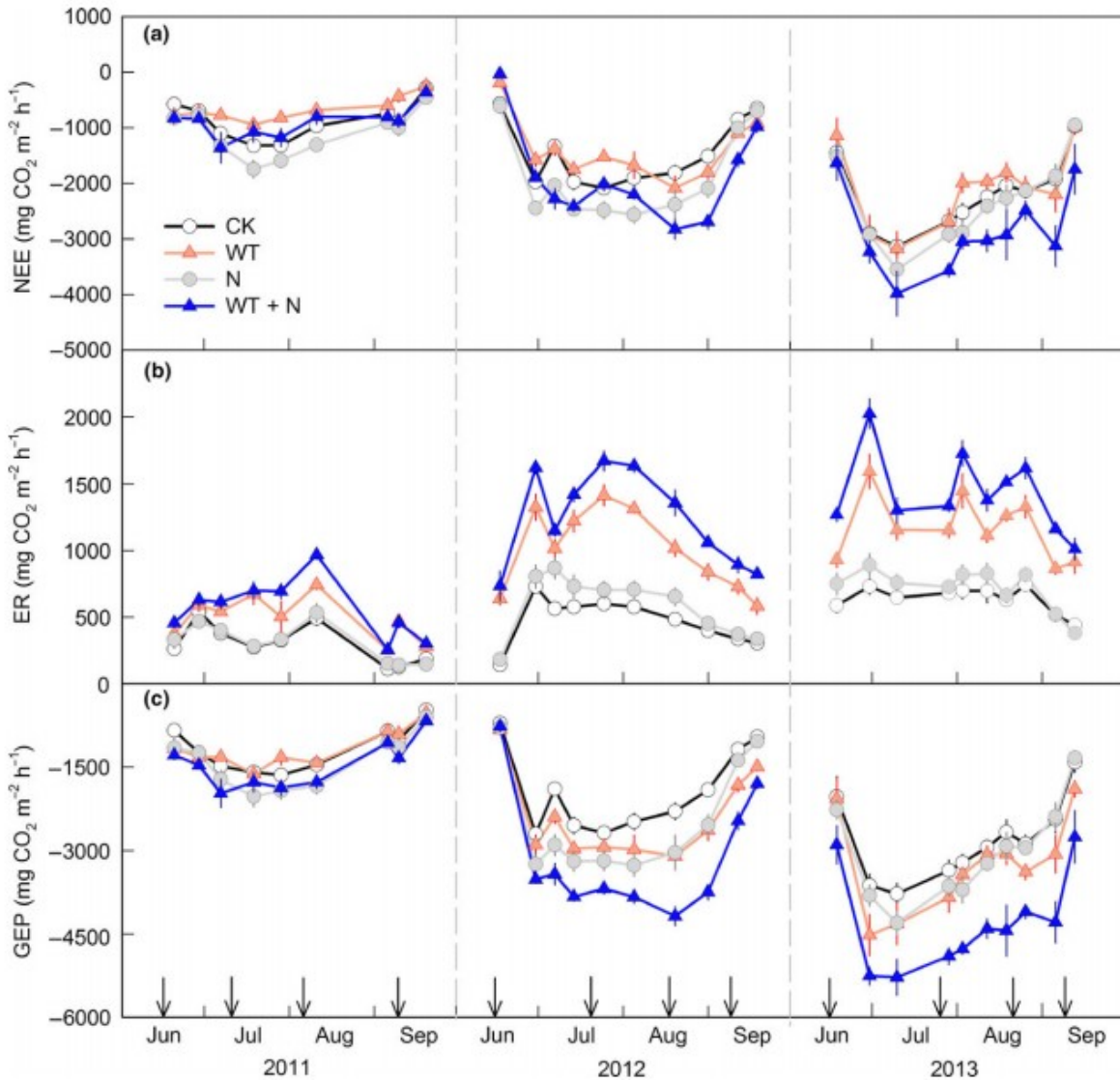

Fig. 3 Seasonal dynamics of daytime (9:00–12:00) average net ecosystem carbon dioxide exchange (NEE) (a), ecosystem respiration (ER) (b) and gross ecosystem productivity (GEP) (c) under different treatments from 2011 to 2013. Bars show ± SE (n = 5). Negative values indicate sinks. The arrows indicate the dates of nitrogen application. CK, control; WT, water table lowering; N, nitrogen deposition; WT + N, combined water table lowering and nitrogen deposition.

Table 1 Repeated-measures ANOVA on the effects of water table lowering, nitrogen deposition, sampling date and their interactions on daytime (9:00–12:00) average carbon dioxide (NEE, net ecosystem carbon dioxide exchange; ER, ecosystem respiration; GEP, gross ecosystem productivity; mg CO_2 m^{-2} h^{-1}), methane (CH_4, mg CH_4 m^{-2} h^{-1}) and nitrous oxide (N_2O, μg N_2O m^{-2} h^{-1}) fluxes during the growing seasons (June–September)

	2011		2012		2013	
	df	F	df	F	df	F
NEE						
WT	1, 16	13.0**	1, 16	0.1	1, 16	2.7
N	1, 16	16.2**	1, 16	32.3***	1, 16	12.7**
WT × N	1, 16	0.01	1, 16	0.3	1, 16	6.1*
Date	8, 128	41.2***	9, 144	173.5***	9, 144	46.5***
Date × WT	8, 128	5.9*	9, 144	15.6***	9, 144	1.7
Date × N	8, 128	1.2	9, 144	8.0*	9, 144	0.9
Date × WT × N	8, 128	1.6	9, 144	0.9	9, 144	0.4
ER						
WT	1, 16	68.3***	1, 16	295.2***	1, 16	186.7***
N	1, 16	2.3	1, 16	23.4***	1, 16	13.4**
WT × N	1, 16	1.4	1, 16	2.9	1, 16	3.8
Date	8, 128	70.9***	9, 144	118.6***	9, 144	47.8***
Date × WT	8, 128	9.4**	9, 144	14.6***	9, 144	11.5**
Date × N	8, 128	1.8	9, 144	1.5	9, 144	2.0
Date × WT × N	8, 128	1.2	9, 144	1.6	9, 144	0.5
GEP						
WT	1, 16	0.1	1, 16	28.3***	1, 16	27.9***
N	1, 16	15.4***	1, 16	33.6***	1, 16	15.7***
WT × N	1, 16	0.3	1, 16	0.9	1, 16	6.7*
Date	8, 128	78.1***	9, 144	286.3***	9, 144	69.5***
Date × WT	8, 128	1.9	9, 144	8.6**	9, 144	1.9
Date × N	8, 128	1.9	9, 144	9.8**	9, 144	0.9
Date × WT × N	8, 128	1.6	9, 144	0.9	9, 144	0.5
CH₄						
WT	1, 16	233.2***	1, 16	301.0***	1, 16	59.8***
N	1, 16	0.3	1, 16	0.1	1, 16	0.8
WT × N	1, 16	4.4	1, 16	4.3	1, 16	0.6
Date	11, 176	11.2**	14, 224	167.6***	8, 128	116.4***
Date × WT	11, 176	29.9***	14, 224	53.7***	8, 128	39.1***
Date × N	11, 176	1.3	14, 224	0.6	8, 128	1.3
Date × WT × N	11, 176	0.7	14, 224	0.9	8, 128	0.5
N₂O						
WT			1, 16	0.3	1, 16	0.03
N			1, 16	41.2***	1, 16	21.8***
WT × N			1, 16	3.3	1, 16	0.8
Date			14, 224	1.3	8, 128	1.9
Date × WT			14, 224	1.2	8, 128	1.5
Date × N			14, 224	1.0	8, 128	1.5
Date × WT × N			14, 224	2.2	8, 128	1.2

WT, N and Date indicate water table, nitrogen deposition and sampling date, respectively. N_2O fluxes were not measured in 2011.
*, ** and ***: statistically significant at $P < 0.05$, $P < 0.01$ and $P < 0.001$.

Table 2 Effects of water table lowering and nitrogen deposition on cumulative carbon dioxide (NEE, net ecosystem carbon dioxide exchange; ER, ecosystem respiration; GEP, gross ecosystem productivity; g CO_2 m^{-2}), methane (CH_4, g CH_4 m^{-2}) and nitrous oxide (N_2O, mg N_2O m^{-2}) fluxes during the growing seasons (June–September)

	NEE		ER		GEP		CH_4		N_2O	
	Mean	SE	Mean	SE	Mean	SE	Mean	SE	Mean	SE
2011										
WT^0	−681.9 b	42.3	823.8 b	48.3	−1505.7 a	80.7	51.0 a	2.6		
WT^-	−551.8 a	33.7	1390.5 a	59.5	−1942.3 b	76.3	16.9 b	1.5		
N^0	−539.6 a	22.8	1039.0 b	92.1	−1578.6 a	76.6	32.8 a	6.9		
N^+	−694.1 b	45.0	1175.3 a	119.2	−1869.4 b	111.2	35.1 a	5.1		
2012										
WT^0	−1114.8 a	60.2	1274.0 b	70.0	−2388.8 a	125.0	49.8 a	1.4	8.3 a	6.1
WT^-	−1068.5 a	59.3	2856.3 a	111.6	−3924.8 b	166.2	23.6 b	0.9	7.6 a	5.2
N^0	−953.1 a	37.0	1853.4 b	239.5	−2806.5 a	237.4	36.6 a	5.1	−3.1 b	3.9
N^+	−1230.2 b	40.3	2276.9 a	298.5	−3507.1 b	301.1	36.8 a	3.9	19.0 a	4.6
2013										
WT^0	−1521.2 a	66.0	1735.7 b	72.2	−3256.9 a	130.1	53.6 a	2.8	15.2 a	10.8
WT^-	−1668.9 a	111.3	3313.3 a	142.1	−4982.2 b	240.8	25.4 b	2.6	21.3 a	14.8
N^0	−1441.2 a	67.2	2308.7 b	241.9	−3749.9 a	257.5	37.7 a	5.9	−7.8 b	4.7
N^+	−1748.9 b	90.5	2740.3 a	307.9	−4489.2 b	379.0	41.2 a	4.9	44.2 a	12.8
Overall										
WT^0	−1106.0 a	50.7	1277.8 b	58.3	−2383.8 a	104.0	51.5 a	1.8	11.7 a	8.0
WT^-	−1096.4 a	61.0	2520.0 a	98.9	−3616.4 b	155.7	21.9 b	1.4	14.4 a	8.8
N^0	−978.0 a	34.8	1733.7 b	188.7	−2711.7 a	186.7	35.7 a	5.8	−5.4 b	3.7
N^+	−1224.4 b	41.2	2064.2 a	239.2	−3288.6 b	257.2	37.7 a	4.5	31.6 a	7.2

WT^0 and WT^- indicate no water table lowering and water table lowering across different nitrogen deposition levels, respectively. N^0 and N^+ indicate no nitrogen deposition and nitrogen deposition across different water table levels, respectively. Different letters indicate significant differences between levels ($n = 10$, $P < 0.05$).

Methane and nitrous oxide fluxes

CH_4 emissions ranged from 33.9 to 39.5 g CH_4 m^{-2} across all treatments in the three years (Fig. 4a). Significant seasonal dynamics ($P < 0.01$) were observed (Table 1), and the highest value appeared in mid-August. WTL substantially reduced CH_4 emissions by 67.0% in 2011, 52.7% in 2012 and 52.7% in 2013 compared with the no-WTL plots, whereas N deposition had no significant effect on CH_4 emissions (Fig. S3a, Table 2).
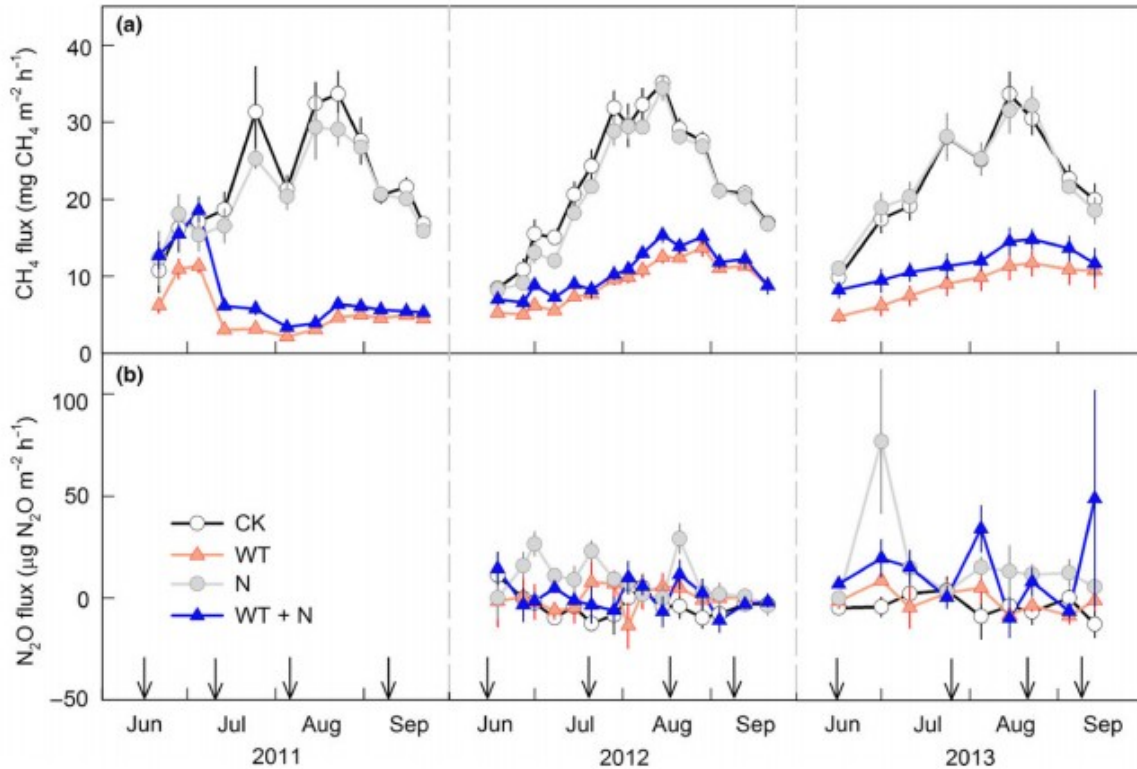
Fig. 4 Seasonal dynamics of daytime (9:00–12:00) average methane fluxes (CH_4) (a) and nitrous oxide fluxes (N_2O) (b) under different treatments from 2011 to 2013. Bars show ± SE ($n = 5$). Negative values indicate sinks. The arrows indicate the dates of nitrogen application. CK, control; WT, water table lowering; N, nitrogen deposition; WT + N, combined water table lowering and nitrogen deposition.

The absorptions of N_2O were weak and varied from -3.4 to -12.9 mg N_2O m^{-2} in the control plots (Fig. 4b). No significant seasonal dynamics were detected (Table 1), and the N_2O fluxes fluctuated around zero. WTL had no significant effect on N_2O fluxes, whereas N deposition significantly increased N_2O release ($P < 0.001$), resulting in net N_2O emissions (Fig. S3b, Table 2). Moreover, no significant WT × N interactions were observed.

Global warming potential

The GWP of growing season GHG budgets ranged from 14.6 to 876.3 g CO_2-eq m^{-2} for the control plots (Fig. 5a). Overall, WTL turned the GWP of this wetland from positive (337.3 g CO_2-eq m^{-2}, warming) to negative (-480.1 g CO_2-eq m^{-2}, cooling) across different N deposition levels, and this change was mainly caused by the decrease in CH_4 emissions (Fig. 5b). Compared with the no-N deposition plots, N deposition reduced the GWP from 21.0 to -163.8 g CO_2-eq m^{-2}, because the increase in net CO_2 uptake exceeded the enhancement in CO_2 equivalents from CH_4 and N_2O emissions (Fig. 5c).
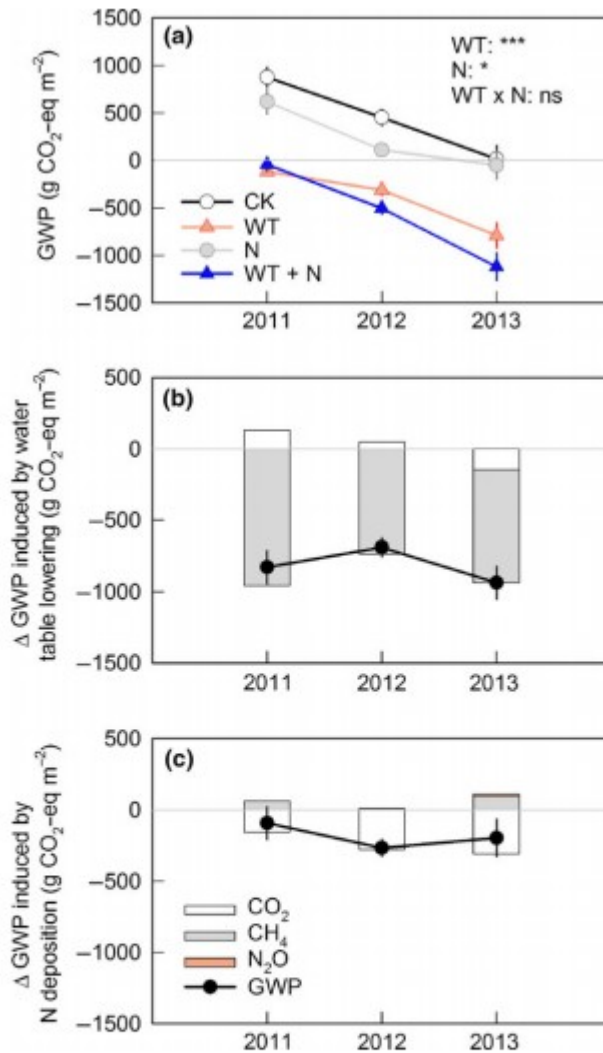
Fig. 5 The global warming potential (GWP) of growing season GHG budgets under different treatments (a) and differences in GWP induced by water table lowering (b) and nitrogen deposition (c). In panel (a), bars show ± SE ($n = 5$); CK, control; WT, water table lowering; N, nitrogen deposition; WT + N, combined water table lowering and nitrogen deposition; ns, * and ***: not statistically significant and statistically significant at $P < 0.05$ and $P < 0.001$. In panels (b) and (c), bars show ± SE ($n = 10$).

Abundance of genes associated with CH$_4$ and N$_2$O fluxes

The abundance of methane-producing gene (*mcrA*) markedly decreased ($P = 0.04$; Fig. 6a), whereas the abundance of methane-oxidizing genes (*pmoA* and *mmoX*) remained unchanged under WTL conditions (Fig. 6b). Similarly, N deposition considerably decreased the abundance of methane-producing genes ($P = 0.08$), but did not affect that of methane-oxidizing genes. These results imply that both WTL and N deposition mainly influence CH$_4$ production potential, rather than CH$_4$ oxidation potential.
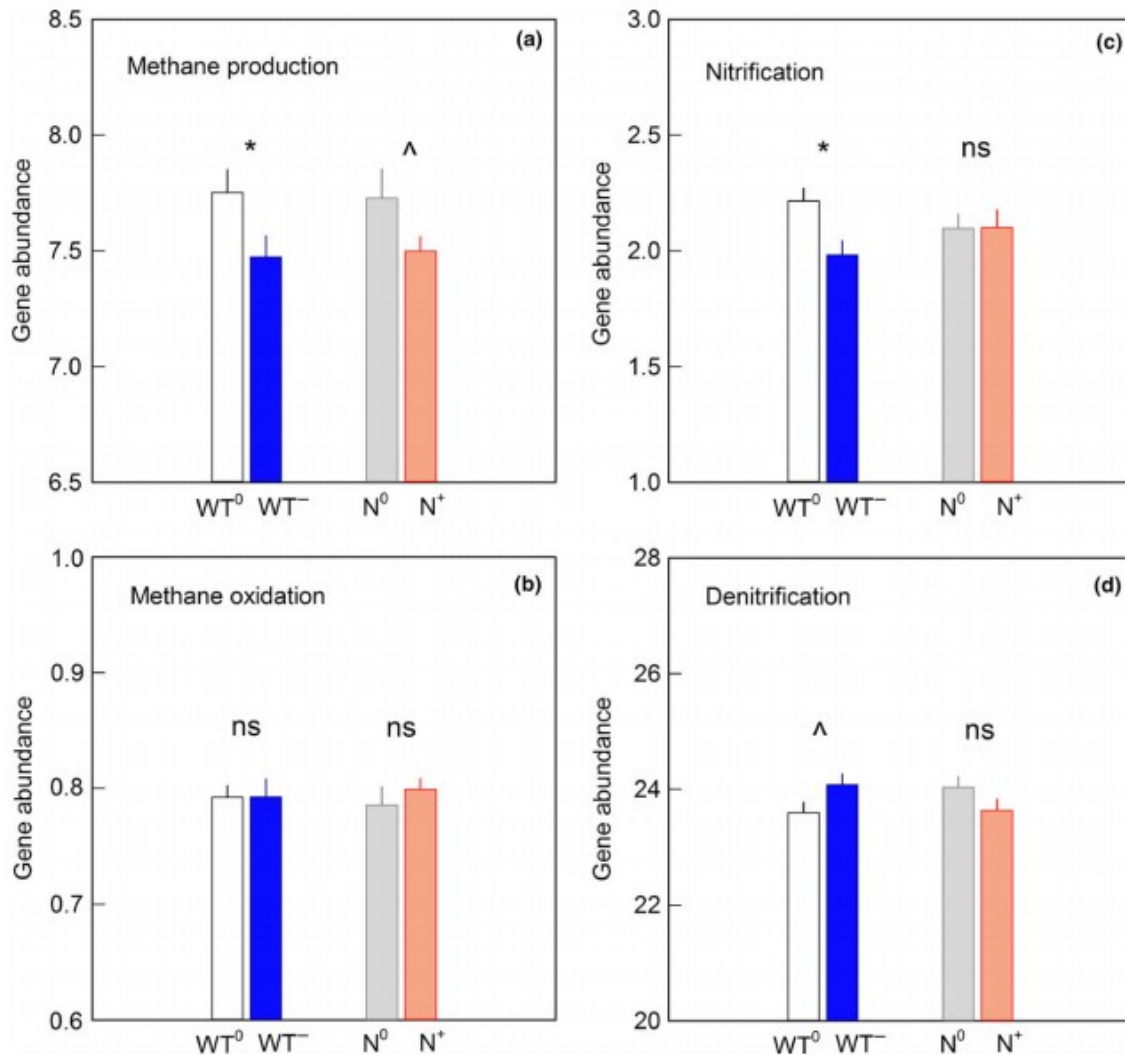
Fig. 6 Effects of water table lowering and nitrogen deposition on the abundance ($\times 10^5$) of genes associated with methane production (a), methane oxidation (b), nitrification (c) and denitrification (d) in September 2013. Bars show $\pm$ SE ($n = 10$). WT^0 and WT^- indicate no water table lowering and water table lowering across different nitrogen deposition levels, respectively. N^0 and N^+ indicate no nitrogen deposition and nitrogen deposition across different water table levels, respectively. ns, ^ and *: not statistically significant and statistically significant at $0.05 < P < 0.1$ and $P < 0.05$.

WTL significantly decreased the abundance of genes (*amoA* and *hao*) involved in nitrification ($P = 0.01$; Fig. 6c), but marginally increased the abundance of genes (*nirS*, *nirK, narG* and *norB*) involved in denitrification ($P = 0.06$; Fig. 6d), suggesting that both nitrification and denitrification potentials were influenced by WTL. More specifically, WTL decreased the abundance of *amoA* or *nirS*, increased the abundance of *narG* and did not affect that of *hao*, *nirK* or *norB* (Fig. S6). N deposition did not affect the abundance of the nitrifying and denitrifying genes.

Discussion

Our results partially support hypotheses I and II; that is, WTL decreases CH_4 emissions and N deposition increases net CO_2 uptake and N_2O emissions. In contrast to our predictions, WTL did not affect net CO_2 uptake or N_2O fluxes,

and N deposition had no effect on CH_4 emissions. Hypothesis III, which states that the effects of WTL on GHG emissions are modulated by N deposition, is not supported. This study shows that both WTL and N deposition reduced the overall GWP although the mechanisms differed. That is, the WTL-induced reduction was mainly caused by decreased CH_4 emissions, whereas the N-induced reduction was largely caused by increased net CO_2 uptake. GeoChip analysis suggests that changes in CH_4 production potential, rather than CH_4 oxidation potential, provided explanation to the variations in net CH_4 emissions, and decreased nitrification potential and increased denitrification potential affected N_2O fluxes under WTL condition in this alpine wetland.

WTL decreased CH_4 emissions but did not affect NEE and N_2O fluxes

This three-year study provides direct evidence that simultaneous increases in ER and GEP led to little NEE response to WTL in this alpine wetland. Despite no detectable change across the three years, the response of NEE to WTL varied with time. In 2011, WTL decreased net CO_2 uptake, which is mainly attributed to increased soil CO_2 emission due to improved aeration (Wang *et al*., 2014b) and decreased water supply for plants (Malone *et al*., 2013). Interestingly, the negative influence of WTL on net CO_2 uptake became positive influence after August 2012. One possible explanation is plant acclimation to WTL. It is well documented that drought increases investment of carbon assimilation to roots (Farooq *et al*., 2009). More deep roots under WTL (Fig. 2c) would enable plants to access water in the subsoil. Another explanation is soil nutrient changes during the experiment. WTL-induced increase in N mineralization may stimulate photosynthetic CO_2 fixation in this low N availability ecosystem (Updegraff *et al*., 1995; Laiho, 2006). In short, this study shows that the effect of WTL on NEE varied with time, and demonstrates the necessity of long-term observations.

WTL substantially decreased CH_4 emissions over the three-year observation period, which is consistent with the finding of mesocosms experiment in Zoige peatlands (Yang *et al*., 2014a). This result is also supported by a study showing that seasonal CH_4 emissions are positively correlated with water table depth using eddy covariance methods in the same wetland (Song *et al*., 2015). Decreased CH_4 emissions can be caused either by inhibition of CH_4 production, or stimulation of CH_4 oxidation, or both. Using GeoChip approach, we further proved that decreased CH_4 production, rather than increased CH_4 oxidation, was responsible for the changes in CH_4 emissions under WTL conditions. The lack of change in CH_4 oxidation may be attributed to the following seasons. First, *Carex pamirensis* with well-developed aerenchyma has a higher capacity in transporting CH_4 to the atmosphere bypassing the oxidized zones of CH_4 consumption (Bridgham *et al*., 2013). Thus, CH_4 oxidation may play a minor role in net CH_4 emission, and improved aeration under WTL conditions led to a limited increase in CH_4 consumption. Second, the low oxygen density at high elevations (3200 m, approximately 70% of that at sea level) can to some extent limit CH_4 oxidation, because low

oxygen availability reduces the activities of methanotrophs (Le Mer & Roger, 2001). Further evidence is required to verify these speculations.

Generally, improved aerobic condition induced by WTL favors N mineralization and subsequent N_2O emissions (Updegraff et al., 1995). Nevertheless, our results show that WTL did not affect N_2O fluxes. This may be attributed to high C/N ratio (16.8) in the 0–30 cm soil layer in this alpine wetland (Song et al., 2015), since high C/N ratio limits the influence of WTL on N_2O emissions, as reported by Klemedtsson et al. (2005). It is well-known that nitrifying bacteria prefer aerobic conditions but denitrifying bacteria prefer anaerobic conditions. However, GeoChip analysis shows, on the one hand, that WTL decreased nitrification potential (amoA; Fig. S6). One explanation is that the alpine sedge negatively influences soil nitrification by competing for soil ammonium. In this present study, WTL increased ANPP and belowground biomass in 2013, thereby stimulating plant uptake of soil available N. Moreover, the alpine sedge prefers ammonium over nitrate (Raab et al., 1999), which may lead to less soil ammonium for nitrifiers. Other explanation is that the WTL-induced decrease in soil moisture reduces the diffusion of soil ammonium, resulting in low nitrification rate, as supported by a previous study (Osborne et al., 2016). On the other hand, GeoChip data show that WTL increased denitrification potential. This may result from the increased availability of soil nitrate because of the stimulating N mineralization under aerobic conditions and the relatively low uptake of the alpine sedge.

N deposition stimulated NEE and N_2O emissions but did not affect CH_4 emissions

N deposition stimulated net CO_2 uptake (Fig. 3a), suggesting that alpine wetlands may sequester more atmospheric CO_2 under N deposition during growing seasons. Notably, the observed changes in NEE may not be applied to future long-term projections, because shifts in plant community composition in the long term can influence the response of NEE to N treatment. For example, Bubier et al. (2007) and Larmola et al. (2013) reported that N addition increases vascular plants but decreases moss, leading to little impact after 5 years and a negative impact after 7 years on net CO_2 sink in an ombrotrophic bog. Hence, it remains unknown how long N-induced stimulation in NEE lasts in this wetland. However, at least in the short term, the increased CO_2 absorption partly compensated for the reduced CO_2 sink in ombrotrophic bogs.

CH_4 emissions were not affected by N deposition in this current study, which may result from the counteraction of direct and indirect influences. The direct influence was the reduced activity of methanogens, as indicated by decreased CH_4 production potential ($P = 0.08$; Fig. 6a). This is supported by the results of an experiment using soil columns in a peatland of the eastern Tibetan Plateau (Gao et al., 2014) showing that N addition inhibits CH_4 emissions. The indirect influence was caused by the increased plant ANPP,

which benefits CH_4 emissions (Hirota *et al*., 2004). Therefore, in the current study, the observed no effect of N deposition on CH_4 emissions is probably a result of a positive effect from plants being offset by a negative effect from microbes.

In the present study, N deposition generally shifted this alpine wetland from a N_2O sink to a N_2O source over the whole growing season, but variations existed in specific sampling period. For instance, no significant changes in N_2O emissions were detected under N deposition in mid-September 2013 (Fig. S3b). Our soil sampling for GeoChip experiment was also in this period. GeoChip data show no changes in nitrification and denitrification potentials, which is consistent with N_2O flux response to N deposition. We acknowledge that this low sampling frequency in GeoChip analysis due to the high cost is a limitation to the understanding of the mechanisms underlying the overall N_2O flux response.

No interactive effects of WTL and N deposition

Concurrent changes in water and N deposition in wetlands challenge the ability to extrapolate GHG responses based on the results of single-factor experiments. This study is among a few studies focusing on the interactions between water and N deposition at the ecosystem scale. For example, WTL stimulates N_2O emissions from nutrient-rich soils in peatlands, but has no impact on emissions from nutrient-poor soils (Martikainen *et al*., 1993; Aerts & Ludwig, 1997). In a California grassland, water addition alone increases net CO_2 uptake, but has no effect under N addition (Harpole *et al*., 2007). However, our finding suggests that N deposition did not alter the effects of WTL on GHG emissions in this alpine wetland. One possible explanation is that stimulated N mineralization increases N availability under WTL conditions in this wetland, thereby overlapping the effect of N deposition. Another explanation is that microbial community structure has changed except for physiological acclimation of microbes, when facing a larger soil water gradient. It has been reported that WTL increases fungi but decreases Gram-negative bacteria in the upper soil of a boreal fen (Jaatinen *et al*., 2007). We speculate that microbes reduce the demand for N because of shifting in community composition after three years of WTL in the current study.

WTL and N deposition both reduced the GWP of GHG emissions

Few studies have quantified the climate impact of alpine wetlands and its response to environmental changes. Using the widely used 100-year GWP, this study estimates that the pristine Tibetan alpine wetlands have a positive net GWP with growing season GHG budgets, that is exerting a net warming impact on global radiation balance. We further found that decreased CH_4 emissions led to reduction in GWP under WTL conditions, as supported by an earlier study in arctic wet tundra (Merbold *et al*., 2009). The weakened CH_4 source strength of alpine wetlands and the corresponding climate impact deserve more attention because the wetland of the Tibetan Plateau is one of

the two largest natural sources of CH_4 in China (Ding *et al*., 2004). By contrast, our results suggest that increased net CO_2 uptake was the dominant contributor to the reduction in GWP following N deposition. This finding is inconsistent with previous studies based on *in situ* experiments (Zhang *et al*., 2013), meta-analyses (Liu & Greaver, 2009) and coupled biogeochemical models (Lu & Tian, 2013), reporting that N-driven stimulation in CH_4 and N_2O emissions increases GWP. This discrepancy is possibly because of the larger responsive intensity of net CO_2 uptake than CH_4 and N_2O emissions in this alpine wetland.

On the Tibetan Plateau, continued climate warming has been projected by the IPCC global climate models, and it has been suggested that climate warming will lead to more permafrost degradation and WTL in typical alpine wetlands (Cheng & Wu, 2007; Trenberth *et al*., 2007). With intensified human activities, N deposition may increase in the near future. We estimated that the reduction in GWP ranged from 919.1 to 1132.5 g CO_2-eq m^{-2} when WTL and N deposition were combined. If we simply extrapolate our results to the alpine wetlands (with the exception of riverine and lacustrine wetlands) of the Tibetan Plateau (6.3×10^4 km^2, Wei *et al*., 2015), approximately 57.9–71.3 Tg CO_2-eq per growing season will be taken up if all Tibetan wetlands are simultaneously subject to WTL and N deposition.

Our study was motivated by the alpine environments of the Tibetan Plateau, which are expected to strongly influence the GHG responses to environmental changes. The low oxygen density, among the unique environments, reduces the activities of methanotrophs. In addition, the alpine sedges acclimate to WTL by allocating more resources to deep roots. Furthermore, the sedge plants are efficient in CH_4 transportation and prefer ammonium over nitrate. Further studies should investigate these mechanisms for the influence of WTL and N deposition on GHG emissions.

It should be noted that wintertime GHG fluxes were not observed due to the harsh conditions of this wetland, which causes an underestimation of annual GHG emissions. However, this underestimation should not affect our general conclusions because the wetland is covered by ice during most of the non-growing season. In addition, we do not have inter-annual data on belowground biomass and soil properties to explain the inter-annual variations in ecosystem-scale GHG responses. These detailed ecosystem-level parameters, although need destructive sampling, warrant further investigation.

Here, for the first time, we examined the net climate impact of three GHG emissions and explored the possible molecular mechanisms underlying the changes in GHG emissions under WTL and N deposition in a Tibetan alpine wetland. Our results reveal that both WTL and N deposition decrease the GWP of GHG emissions by affecting different gas species. More importantly, the variances in microbial functional genes are aligned with the changes in ecosystem-scale GHG emissions. Our results suggest that microbial

mechanisms should be considered when predicting ecosystem-scale GHG responses to future environmental changes.

References

Aerts R, Ludwig F (1997) Water-table changes and nutritional status affect trace gas emissions from laboratory columns of peatland soils. *Soil Biology and Biochemistry*, 29, 1691– 1698.

An S, Li H, Guan B *et al*. (2007) China's natural wetlands: past problems, current status, and future challenges. *Ambio*, 36, 335– 342.

Aurela M, Riutta T, Laurila T *et al*. (2007) CO_2 exchange of a sedge fen in southern Finland—the impact of a drought period. *Tellus Series B*, 59, 826– 837.

Bragazza L, Freeman C, Jones T *et al*. (2006) Atmospheric nitrogen deposition promotes carbon loss from peat bogs. *Proceedings of the National Academy of Sciences of the United States of America*, 103, 19386– 19389.

Bridgham SD, Cadillo-Quiroz H, Keller JK, Zhuang QL (2013) Methane emissions from wetlands: biogeochemical, microbial, and modeling perspectives from local to global scales. *Global Change Biology*, 19, 1325– 1346.

Bubier JL, Moore TR, Bledzki LA (2007) Effects of nutrient addition on vegetation and carbon cycling in an ombrotrophic bog. *Global Change Biology*, 13, 1168– 1186.

Chen H, Yao S, Wu N *et al*. (2008) Determinants influencing seasonal variations of methane emissions from alpine wetlands in Zoige Plateau and their implications. *Journal of Geophysical Research*, 113, D12303.

Chen H, Wu N, Gao Y, Wang Y, Luo P, Tian J (2009) Spatial variations on methane emissions from Zoige alpine wetlands of Southwest China. *Science of the Total Environment*, 407, 1097– 1104.

Chen H, Zhu Q, Peng C *et al*. (2013) The impacts of climate change and human activities on biogeochemical cycles on the Qinghai-Tibetan Plateau. *Global Change Biology*, 19, 2940– 2955.

Cheng G, Wu T (2007) Responses of permafrost to climate change and their environmental significance, Qinghai-Tibet Plateau. *Journal of Geophysical Research*, 112, F02S03.

Chivers MR, Turetsky MR, Waddington JM, Harden JW, Mcguire AD (2009) Effects of experimental water table and temperature manipulations on ecosystem CO_2 fluxes in an Alaskan rich fen. *Ecosystems*, 12, 1329– 1342.

Csonka LN (1989) Physiological and genetic responses of bacteria to osmotic stress. *Microbiological Reviews*, 53, 121– 147.

Dalal RC, Wang WJ, Robertson GP, Parton WJ (2003) Nitrous oxide emission from Australian agricultural lands and mitigation option: a review. *Australian Journal of Soil Research*, 41, 165– 195.

Dijkstra FA, Morgan JA, Follett RF, Lecain DR (2013) Climate change reduces the net sink of CH_4 and N_2O in a semiarid grassland. *Global Change Biology*, 19, 1816– 1826.

Ding WX, Cai ZC, Wang DX (2004) Preliminary budget of methane emissions from natural wetlands in China. *Atmospheric Environment*, 38, 751– 759.

Dinsmore KJ, Skiba UM, Billett MF, Rees RM (2009) Effect of water table on greenhouse gas emissions from peatland mesocosms. *Plant and Soil*, 318, 229– 242.

Dise NB (2009) Peatland response to global change. *Science*, 326, 810– 811.

Fang H, Cheng S, Yu G *et al*. (2012) Responses of CO_2 efflux from an alpine meadow soil on the Qinghai Tibetan Plateau to multi-form and low-level N addition. *Plant and Soil*, 351, 177– 190.

Farooq M, Wahid A, Kobayashi N, Fujita D, Basra S (2009) Plant drought stress: effects, mechanisms and management. *Agronomy for Sustainable Development*, 29, 185– 212.

Frolking S, Roulet N, Fuglestvedt J (2006) How northern peatlands influence the Earth's radiative budget: sustained methane emission vs. sustained carbon sequestration. *Journal of Geophysical Research*, 111, G01008.

Gao Y, Chen H, Zeng X (2014) Effects of nitrogen and sulfur deposition on CH_4 and N_2O fluxes in high-altitude peatland soil under different water tables in the Tibetan Plateau. *Soil Science and Plant Nutrition*, 60, 404– 410.

Goldberg SD, Knorr K-H, Blodau C, Lischeid G, Gebauer G (2010) Impact of altering the water table height of an acidic fen on N_2O and NO fluxes and soil concentrations. *Global Change Biology*, 16, 220– 233.

Harpole WS, Potts DL, Suding KN (2007) Ecosystem responses to water and nitrogen amendment in a California grassland. *Global Change Biology*, 13, 2341– 2348.

Hirota M, Tang Y, Hu Q *et al.* (2004) Methane emissions from different vegetation zones in a Qinghai-Tibetan Plateau wetland. *Soil Biology and Biochemistry*, 36, 737– 748.

IPCC. (2013) *Climate Change 2013: The Physical Science Basis. Contribution of Working Group I to the Fifth Assessment Report of the Intergovernmental Panel on Climate Change*. Cambridge University Press, Cambridge, UK and New York, NY, USA.

Jaatinen K, Fritze H, Laine J, Laiho R (2007) Effects of short- and long-term water-level drawdown on the populations and activity of aerobic decomposers in a boreal peatland. *Global Change Biology*, 13, 491– 510.

Joabsson A, Christensen TR, Wallen B (1999) Vascular plant controls on methane emissions from northern peatforming wetlands. *Trends in Ecology and Evolution*, 14, 385– 388.

Karbin S, Guillet C, Kammann C, Niklaus P (2015) Effects of long-term CO_2 enrichment on soil-atmosphere CH_4 fluxes and the spatial micro-distribution of methanotrophic bacteria. *PLoS ONE*, 10, e0131665.

Klemedtsson L, Von Arnold K, Weslien P, Gundersen P (2005) Soil CN ratio as a scalar parameter to predict nitrous oxide emissions. *Global Change Biology*, 11, 1142– 1147.

Lai DYF, Moore TR, Roulet NT (2014) Spatial and temporal variations of methane flux measured by autochambers in a temperate ombrotrophic peatland. *Journal of Geophysical Research: Biogeosciences*, 119, 864– 880.

Laiho R (2006) Decomposition in peatlands: reconciling seemingly contrasting results on the impacts of lowered water levels. *Soil Biology and Biochemistry*, 38, 2011– 2024.

Larmola T, Bubier JL, Kobyljanec C *et al.* (2013) Vegetation feedbacks of nutrient addition lead to a weaker carbon sink in an ombrotrophic bog. *Global Change Biology*, 19, 3729– 3739.

Le Mer J, Roger P (2001) Production, oxidation, emission and consumption of methane by soils: a review. *European Journal of Soil Biology*, 37, 25– 50.

Lebauer DS, Treseder KK (2008) Nitrogen limitation of net primary productivity in terrestrial ecosystems is globally distributed. *Ecology*, 89, 371– 379.

Liu L, Greaver TL (2009) A review of nitrogen enrichment effects on three biogenic GHGs: the CO_2 sink may be largely offset by stimulated N_2O and CH_4 emission. *Ecology Letters*, 12, 1103– 1117.

Liu Y, Xu-Ri WY, Pan Y, Piao S (2015) Wet deposition of atmospheric inorganic nitrogen at five remote sites in the Tibetan Plateau. *Atmospheric Chemistry and Physics*, 15, 11683– 11700.

Lohila A, Aurela M, Hatakka J, Pihlatie M, Minkkinen K, Penttilä T, Laurila T (2010) Responses of N_2O fluxes to temperature, water table and N deposition in a northern boreal fen. *European Journal of Soil Science*, 61, 651– 661.

Lu C, Tian H (2007) Spatial and temporal patterns of nitrogen deposition in China: synthesis of observational data. *Journal of Geophysical Research*, 112, D22S05.

Lu C, Tian H (2013) Net greenhouse gas balance in response to nitrogen enrichment: perspectives from a coupled biogeochemical model. *Global Change Biology*, 19, 571– 588.

Luton PE, Wayne JM, Sharp RJ, Riley PW (2002) The *mcrA* gene as an alternative to 16S rRNA in the phylogenetic analysis of methanogen populations in landfill. *Microbiology*, 148, 3521– 3530.

Malone SL, Starr G, Staudhammer CL, Ryan MG (2013) Effects of simulated drought on the carbon balance of Everglades short-hydroperiod marsh. *Global Change Biology*, 19, 2511– 2523.

Martikainen PJ, Nykanen H, Crill P, Silvola J (1993) Effect of a lowered water table on nitrous oxide fluxes from northern peatlands. *Nature*, 366, 51– 53.

McCalley CK, Woodcroft BJ, Hodgkins SB *et al*. (2014) Methane dynamics regulated by microbial community response to permafrost thaw. *Nature*, 514, 478– 481.

Merbold L, Kutsch WL, Corradi C *et al*. (2009) Artificial drainage and associated carbon fluxes (CO_2/CH_4) in a tundra ecosystem. *Global Change Biology*, 15, 2599– 2614.

Niu S, Wu M, Han Y, Xia J, Li L, Wan S (2008) Water-mediated responses of ecosystem carbon fluxes to climatic change in a temperate steppe. *New Phytologist*, 177, 209– 219.

Osborne BB, Baron JS, Wallenstein MD (2016) Moisture and temperature controls on nitrification differ among ammonia oxidizer communities from three alpine soil habitats. *Frontiers of Earth Science*, 10, 1– 12.

Petrescu AMR, Lohila A, Tuovinen J-P *et al*. (2015) The uncertain climate footprint of wetlands under human pressure. *Proceedings of the National Academy of Sciences of the United States of America*, 112, 4594– 4599.

Piao S, Ciais P, Huang Y *et al*. (2010) The impacts of climate change on water resources and agriculture in China. *Nature*, 467, 43– 51.

Raab TK, Lipson DA, Monson RK (1999) Soil amino acid utilization among species of the Cyperaceae: plant and soil processes. *Ecology*, 80, 2408– 2419.

Schimel J, Balser TC, Wallenstein M (2007) Microbial stress-response physiology and its implications for ecosystem function. *Ecology*, 88, 1386– 1394.

Smith KA, Ball T, Conen F, Dobbie KE, Massheder J, Rey A (2003) Exchange of greenhouse gases between soil and atmosphere: interactions of soil physical factors and biological processes. *European Journal of Soil Science*, 54, 779– 791.

Song WM, Wang H, Wang GS, Chen LT, Jin ZN, Zhuang QL, He J-S (2015) Methane emissions from an alpine wetland on the Tibetan Plateau: neglected but vital contribution of the nongrowing season. *Journal of Geophysical Research*, 120, 1475– 1490, doi:10.1002/2015JG003043.

Trenberth KE, Jones PD, Ambenje P *et al*. (2007) Observations: surface and atmospheric climate change. In: *Climate Change 2007: The Physical Science Basis. Contribution of Working Group I to the Fourth Assessment Report of the Intergovernmental Panel on Climate Change* (eds S Solomon, D Qin, M Manning, Z Chen, M Marquis, KB Averyt, M Tignor, HL Miller), pp. 237– 336. Cambridge, UK and New York, NY, USA.

Updegraff K, Pastor J, Bridgham SD, Johnston CA (1995) Environmental and substrate controls over carbon and nitrogen mineralization in northern wetlands. *Ecological Applications*, 5, 151– 163.

Wang YS, Wang YH (2003) Quick measurement of CH_4, CO_2 and N_2O emissions from a short-plant ecosystem. *Advances in Atmospheric Sciences*, 20, 842– 844.

Wang S, Duan J, Xu G *et al*. (2012) Effects of warming and grazing on soil N availability, species composition, and ANPP in an alpine meadow. *Ecology*, 93, 2365– 2376.

Wang C, Wang X, Liu D *et al*. (2014a) Aridity threshold in controlling ecosystem nitrogen cycling in arid and semi-arid grasslands. *Nature Communications*, 5, 4799.

Wang H, Yu LF, Chen LT, Wang C, He J-S (2014b) Responses of soil respiration to reduced water table and nitrogen addition in an alpine wetland on the Qinghai-Xizang Plateau. *Chinese Journal of Plant Ecology*, 38, 619– 625, in Chinese with an English abstract.

Webster KL, Mclaughlin JW, Kim Y, Packalen MS, Li CS (2013) Modelling carbon dynamics and response to environmental change along a boreal fen nutrient gradient. *Ecological Modelling*, 248, 148– 164.

Wei D, Xu-Ri TT, Dai D, Wang Y, Wang Y (2015) Revisiting the role of CH_4 emissions from alpine wetlands on the Tibetan Plateau: evidence from two *in situ* measurements at 4758 and 4320 m above sea level. *Journal of Geophysical Research: Biogeosciences*, 120, 1741– 1750.

Yang J, Liu J, Hu X, Li X, Wang Y, Li H (2013) Effect of water table level on CO_2, CH_4 and N_2O emissions in a freshwater marsh of Northeast China. *Soil Biology and Biochemistry*, 61, 52– 60.

Yang G, Chen H, Wu N *et al*. (2014a) Effects of soil warming, rainfall reduction and water table level on CH$_4$ emissions from the Zoige peatland in China. *Soil Biology and Biochemistry*, 78, 83– 89.

Yang Y, Gao Y, Wang S *et al*. (2014b) The microbial gene diversity along an elevation gradient of the Tibetan grassland. *ISME Journal*, 8, 430– 440.

Yerbury JJ, Stewart EM, Wyatt AR, Wilson MR (2005) Quality control of protein folding in extracellular space. *EMBO Reports*, 6, 1131– 1136.

Yu L, Wang H, Wang G *et al*. (2013) A comparison of methane emission measurements using Eddy Covariance and manual and automated chamber-based techniques in Tibetan Plateau alpine wetland. *Environmental Pollution*, 181, 81– 90.

Yuan J, Ding W, Liu D, Kang H, Freeman C, Xiang J, Lin Y (2015) Exotic *Spartina alterniflora* invasion alters ecosystem-atmosphere exchange of CH$_4$ and N$_2$O and carbon sequestration in a coastal salt marsh in China. *Global Change Biology*, 21, 1567– 1580.

Yue H, Wang M, Wang S *et al*. (2015) The microbe-mediated mechanisms affecting topsoil carbon stock in Tibetan grasslands. *ISME Journal*, 9, 2012– 2020.

Zhang X, Liu H, Xing Z (2011a) Challenges and solutions for sustainable land use in Ruoergai-the highest altitude peatland in Qinhai-Tibetan Plateau, China. *2010 International Conference on Energy, Environment and Development (Iceed2010)*, 5, 1019– 1025.

Zhang Y, Wang G, Wang Y (2011b) Changes in alpine wetland ecosystems of the Qinghai-Tibetan plateau from 1967 to 2004. *Environmental Monitoring and Assessment*, 180, 189– 199.

Zhang L, Song C, Nkrumah PN (2013) Responses of ecosystem carbon dioxide exchange to nitrogen addition in a freshwater marshland in Sanjiang Plain, Northeast China. *Environmental Pollution*, 180, 55– 62.